

Flow Visualization Study of Wing-Tip Vortex for a Wing with Cavity

Tey Shen Xi, Noorfazreena Mohammad Kamaruddin and Zulfaa Mohamed-Kassim
School of Aerospace Engineering, Universiti Sains Malaysia,
14300 Nibong Tebal, Penang, Malaysia

Abstract: This study investigates the flow structures of wing-tip vortex for a wing model with cavity variation at low Reynolds number. The flow structures over a triple-cavities wing model with an aspect ratio of 2 were investigated at angle of attack 0° , 5° , 10° and 15° by using smoke wire flow visualization technique. A non-cavity flat plate model was employed as a reference for comparison of flow structures between the two wing models. The flow visualization results revealed that as the angle of attack increased the wing-tip vortices were increased in strength and more maturely developed with an inboard circulation over the wing-tip. The downwash effect of the wing-tip vortex also resulted in vortex trapping in the cavity of the wing model which rotated clockwise before exiting the cavity. The experiment also revealed that the vortex is trapped and occurred more significantly at higher angle of attack which could potentially lead to the reduction of induced drag.

Key words: Wing-tip vortex, cavity, smoke visualization technique, vortex trapping, wing model

INTRODUCTION

Wing-tip vortices have the potential of imposing flight safety hazards (Gerz *et al.*, 2002). Wing-tip vortices from large aircraft are susceptible to leaving wake vortex turbulence which may persist for minutes after their generations. If a trailing aircraft penetrates the wake it could potentially be a flight safety issue due to the induced roll on the airplane created by the circulation of the vortex. In the aviation history, numerous incident reports on wake vortex turbulence have been filed over the decades. Rossow *et al.* (1995) reported these flight safety issues are related to wake vortex turbulence consist of the separation distances between aircraft. In the recent years where air traffic volume has been increasing due to the growth in passenger's demands and the emergence of low-cost carriers the increase in air traffic requires higher frequencies of take-off and landing. This implies higher occurrence of wake vortex accidents due to higher possibility of wake vortex encounter and because tip vortex circulation is maximal when an aircraft is taking off or landing (Elsayed *et al.*, 2009; Arndt *et al.*, 1991).

Wing with cavity has the potential to enhance lift and reduce induced drag as a direct result of the reduction of wing-tip vortex strength (Sohn and Chang, 2012). At the same time, it also has the potential to replace the high lift devices particularly for low aspect ratio wing aircraft. In a contrary to high lift devices, cavity wing model has the advantages of reductions in structural weight and complexity of mechanism.

Throughout the last decade, numerous researches and experiments were carried out to study the flow structures of wing-tip vortices due to its potential hazardous effects to aircraft. Giuni and Green (2013) have researched on vortex formation for squared and rounded tip and revealed that the wing with squared tips present two sharp edges and produce a multiple vortex structure with highly unsteady secondary vortices. Comparatively, a vortex formed by a wing with rounded tip presents fewer and less intense secondary vortices.

The physical characteristics of wing tip play a role in altering the behavior of wing-tip vortex. Sohn and Chang (2012) performed smoke-wire visualization on a half-wing model with an aspect ratio of 3.2 and 3 different wing configurations namely, square-cut, simple fairing and Whitcomb's full winglet wingtip at angles of attack of $\alpha = 2^\circ$, 10° and 20° . The flow visualization experiment was performed at Reynolds number of 5.5×10^4 . Sohn and Chang (2012) revealed that the wing-tip vortices of the Whitcomb's winglet configuration were reduced in strength and displaced outboard and upward in the near wake region. A comparison of aerodynamic loads between the simple fairing and the Whitcomb's winglet configurations then revealed an increase in the lift coefficient of the winglet configuration by 9% at angle of attack of 10° . The increase in the lift coefficient of the winglet configuration has two sources, namely, the increase in the effective wing area and the decrease in the downwash resulting from the weakening of the wing-tip vortex (Sohn and Chang, 2012).

For low aspect ratio aircraft ($AR < 3$), Liu and Hsiao (2012) have concluded from experimental work for flat plate wing at Reynolds numbers between 10^4 and 10^5 that the high stall angle of attack and vortex lift are manifested to induce an increase in the lift as the aspect ratio reaches < 1.6 . Liu and Hsiao (2012) also indicated that the wing-tip vortices and the areas of highly affected regions are duly increased with the increase of the angle of attack up to 40° . This research outcome is particularly practical to the planform design of unmanned aerial vehicles (Liu and Hsiao, 2012).

Giuni and Green (2013) and Sohn and Chang (2012) demonstrated that the geometrical and physical characteristics of a wing-tip have direct effects on the flow structures of wing-tip vortices. In this present study, the wing model with cavity has distinct physical differences including wing total surface area and physical configuration as compared to non-cavity wing model, hence the flow structures of wing-tip vortices produced by wing model with cavity also varied from that produced by non-cavity wing model. Sohan and Chang (2012) experimental results revealed that wing-tips of different physical configurations have distinct flow structures and vortex intensities. As a consequence, the lift and drag coefficients resulted from the respective wing-tip configurations also varied. In this current study, the presence of cavity on a wing model changed the physical characteristics of a wing model; this implied that different flow structures and wing-tip vortex intensity were exhibited by the cavity wing model and the non-cavity wing model. The alteration in the intensity of flow structures of wing-tip vortices is paramount in this present study due to its potential influence on the lift-to-drag ratio of the wing model which can be explored quantitatively in the future work.

The objective of this present study is to investigate the behavior of wing-tip vortex for a wing with cavity on a flat plate model by using a smoke wire flow visualization technique in a low speed closed-loop wind tunnel. The flow structures around the wing-tip of a baseline (no-cavity) wing and a flat plate model with triple cavities were visualized from side view and rear view at angles of attack, or $\alpha = 0^\circ, 5^\circ, 10^\circ$ and 15° . The experiment was conducted at a flow speed of 1.5 m/sec corresponding to Reynolds number of 25,808. The flow visualization results were analyzed in terms of the intensity and the flow structures of the wing-tip vortices.

MATERIALS AND METHODS

The experiment facilities in this study include a low-speed closed circuit wind tunnel and a smoke visualization system. The wind tunnel with a contraction ratio of 10:1 has a test section of $1.0 \times 0.8 \times 1.8$ m and a maximum achievable speed of 80 m/sec. The wing models

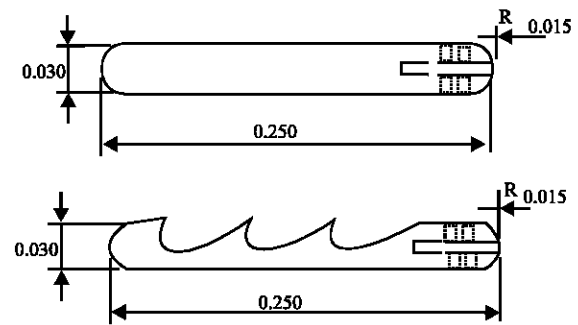


Fig. 1: Cross section views of the wings with no cavity (top) and triple cavities (bottom). Units were listed in metres (Tee, 2015)

tested in this study consist of a triple-cavity flat plate wing model to visualize the flow structures on a multiple cavities wing model hence the single cavity effect is not considered in this research. A non-cavity flat plate model was used for reference for comparison of flow structures between the two wing models. Both of the wing models have an aspect ratio of 2, wing span of 0.5 m, wing chord of 0.25 m and wing thickness of 0.030 m. All of the cavity designs of the triple-cavity wing model have a length-to-depth ratio of 2.75 with the distance between cusp to cusp of 55 mm and a maximum depth of 0.020 m. The ratio of the horizontal curvature length to the vertical height ratio for the first cusp design was 7.5 with vertical height of 2.8 mm measured from the upper surface of flat plate wing. The flat plate wing models were made of Aluminium for smooth finishing surface and the wing model surfaces were coated with black matte paint to prevent strong light reflection. Figure 1 detailed the dimensions of the wing models.

The wing model is mounted horizontally in the wind tunnel test section. A 0.25 mm diameter Nichrome wire is stretched vertically and is positioned upstream from the target flow field about 45 mm inbound of the wing-tip (Sohan and Chang, 2011). When the airflow speed achieves its steady state, a syringe filled with Safex oil is used to manually drip the oil onto the wire from the top of the wind tunnel test section. The wire is heated with a power supply of 30 V, 3 A to generate smoke streak lines (Tee, 2015).

Two 240 V, 50 W yellow halogen light bulbs were used to illuminate the smoke streak lines. The wind tunnel motor was set to run at 41 RPM with a corresponding air velocity of about 1.5 m/sec. The flow structures were captured at angles of attack of $0^\circ, 5^\circ, 10^\circ$ and 15° . The flow structures were recorded using a video camera with resolution of 1920×2080 HD. Figure 2 shows the side view of the experimental setup. The experimental setup from the top of the wind tunnel test section is shown in Fig. 3.

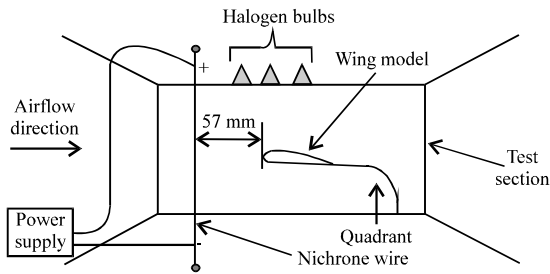


Fig. 2: Side view of the smoke visualization system setup (Tee, 2015)

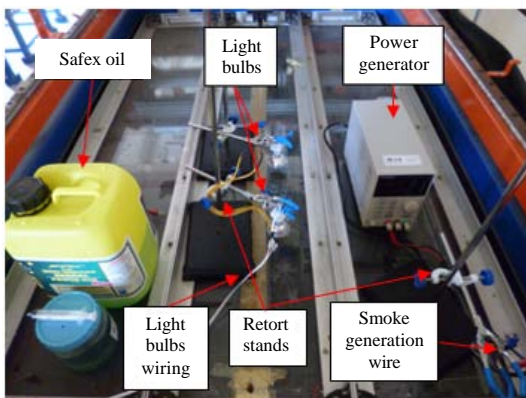


Fig. 3: Experimental setup from the top of the wind tunnel test section

RESULTS AND DISCUSSION

The smoke wire flow visualization experiment revealed interesting behaviors of the flow around the wing-tip of the triple-cavities wing model at different angles of attack. Figure 4-7 show the flow structures of the wing-tip vortices viewed from the side and rear of the non-cavity and the triple-cavity wing models at $\alpha = 0^\circ, 5^\circ, 10^\circ$ and 15° , respectively. The smoke streak lines flow from the left to the right side of the images for side view configuration and from inward towards outward for images on rear view configuration.

At zero angle of attack (Fig. 4) the smoke streak lines remained streamlines and no curling of flow at the wing-tip is observed for both of the wing models. Figure 4a-d also revealed that no tip leaking smoke streak lines appeared for both of the wing models at zero angle of attack. When the flow structures are viewed from the side of the wing models (Fig. 4-d) it is observed that no vortex was trapped at either of the cavities when the triple-cavity wing model was positioned at zero angle of attack.

Due to the symmetric feature of the flat plate wing model, there is no pressure difference between the upper

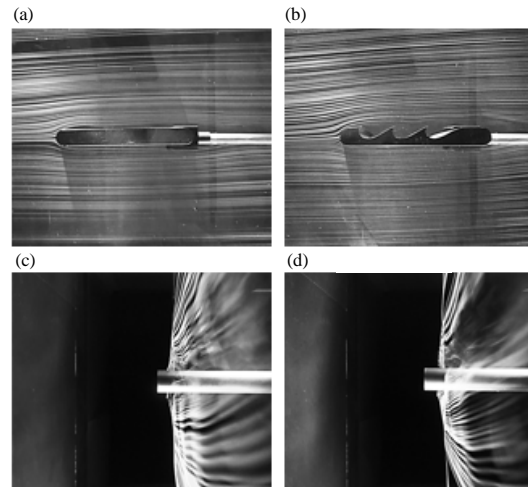


Fig. 4: Flow structures of wing-tip vortex from: a) Side view; b) Rear view at AOA of 0° for; c) Non-cavity flat plate and d) Triple-cavities flat plate model

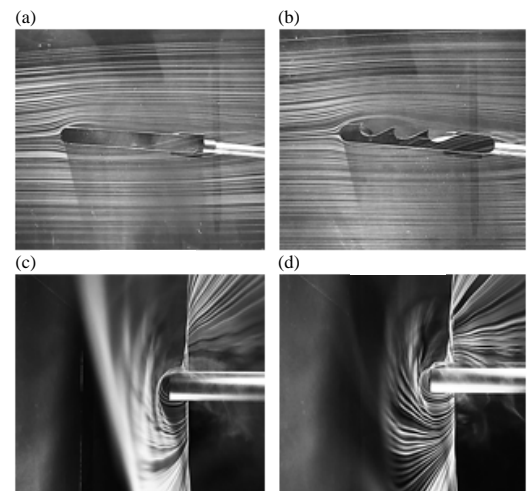


Fig. 5: Flow structures of wing-tip vortex from: a) Side view; b) Rear view at AOA of 5° for; c) Non-cavity flat plate and d) Triple-cavities flat plate model

wing surface and the lower wing surface at zero angle of attack, therefore no wing-tip vortex is formed at zero angle of attack for both of the wing models. Hence, the smoke streak lines appeared smooth and in-plane in the streamwise direction without tip leaking as seen from the rear view in Fig. 4a-d. When the angle of attack was increased to $5^\circ, 10^\circ$ and 15° as shown in Fig. 5-7, respectively, the images clearly indicate curling of the smoke streak lines developed at the wing-tip of the wing

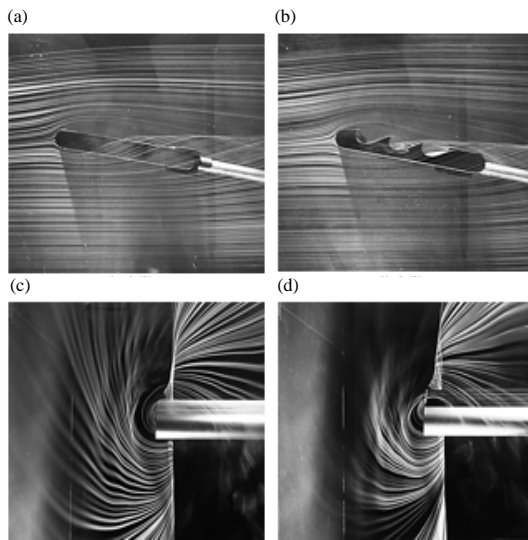


Fig. 6: Flow structures of wing-tip vortex from: a) Side view; b) Rear view at AOA of 10° for; c) Non-cavity flat plate and d) Triple-cavities flat plate model

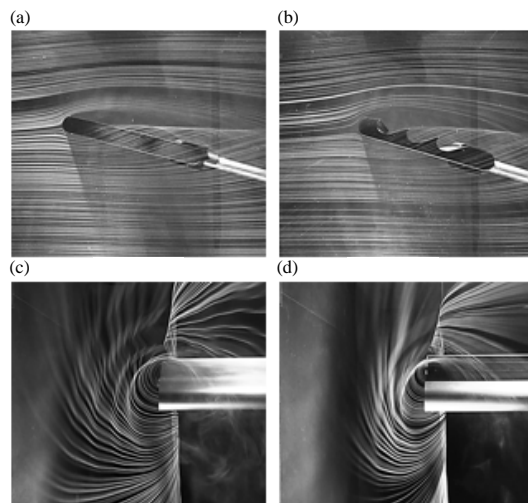


Fig. 7: Flow structures of wing-tip vortex from: a) Side view; b) Rear view at AOA of 15° for; c) Non-cavity flat plate and d) Triple-cavities flat plate model

models. The smoke streak lines have interweaving pattern at the wing-tip trailing edge at non-zero angles of attack. The flow structures in Fig. 5-7a-d suggested that the smoke streak lines curl from the lower side of the wing to upper side of the wing. At angle of attack of 5° , it is observed in Fig. 5a-d that the curling of smoke streak lines started near the trailing edge region. The development of curling elevated as the angle of attack increased. At 15°

angle of attack, most of the wing-tip was covered with the smoke streak lines that curled from the lower wing region to the upper wing region.

Another unique difference of flow structures at zero angles of attack and at non-zero angles of attack can be observed from the rear view of the wing models (Fig. 5-7a-d). The circulatory motion of the wing-tip vortex appeared to expand from the wing-tip section and form a spiral trajectory as the smoke streak lines progressed downstream. At 5° angle of attack, the circulatory motion of the smoke streak lines was less apparent as shown in Fig. 5a-d. Despite the presence of cavities on cavity flat plate model, the flow structures exhibited similar characteristics as that of non-cavity flat plate model. However, an interesting remark of the experimental results is observed in Fig. 5-7a-d for the triple-cavity wing model where at non-zero angles of attack, cavity vortex trapping occurred due to the curling motion of the flow around the wing-tip. At 5° angle of attack, the cavity vortex trapping was captured in the third cavity from the leading edge whereas at 10° and 15° angles of attack as shown in Fig. 6 and 7a the cavity vortex trapping took place in the second cavity.

The increase in angle of attack from 0° - 15° visualized an increase in the interweaving pattern when the flow trailed downstream of the wing model. At 5° angle of attack, the spiral trajectory started to establish with the core of the curling of smoke streak lines remained closely attached to the wing-tip Fig. 5a-d. As the angle of attack increases, the spiral trajectory became more maturely developed as in Fig. 6-7a-d. The core of the spiral trajectory appeared larger as the wing models pitched from 5° - 15° . Correspondingly from the rear view of the wing models, the lower wing surface flow structures curl outboard and upward while the upper wing surface flow structures appeared to bend inboard and downward. As a result, interweaving patterns were formed by the flow structures as seen from the side view of the wing models. Sohn and Chang (2012) examined the wing-tip vortex in the near field of a square-cut wing-tip and reported the spiraling flow of the wing-tip vortex from the higher pressure region wing surface to the lower pressure region surface. In this present study, the inboard circulation of the wing-tip vortex is also observed in Fig. 5-7a-d.

At 5° angle of attack, no flow separation occurred for non-cavity wing model at the upper wing surface but for triple-cavities wing model, the flow separated from the leading edge due to the cavity design and the flow was reattached to the wing model at the middle chord. When the angle of attack increased to 10° and 15° , respectively, flow separation occurred at both of the wing model's leading edges and the flow reattachment was delayed.

In a contrary to the flow structure for the triple-cavities wing model at zero angle of attack, the flow structures at 5° angles of attack were occasionally trapped inside the third cavity from the leading edge due to the roll-up swirling motion of the wing-tip vortex. As a result, the downwash of the wing-tip vortex was trapped inside the cavity and rotated clockwise before exiting the cavity. At 10° and 15° angles of attack, vortex trapping occurred more significantly in the second cavity and is evidently captured in Fig. 6a and b. This occurrence is mainly due to roll-up swirling motion of the wing-tip vortex which was formed closer to the leading edge compared to that at 5° angle of attack.

CONCLUSION

This study investigated the effect of cavity variation on a flat plate wing model on the behavior of wing-tip vortex at angles of attack of 0°, 5°, 10° and 15°. The experiment was conducted at a flow speed of 1.5 m/sec with the corresponding Reynolds number 25,808 using a smoke-visualization system in a wind tunnel. The flow structures of wing-tip vortices of non-cavity and triple-cavity flat plate models were visualized from the side and rear views of the wing models.

The results revealed that the wing-tip vortices exhibited different characteristics at different angles of attack and cavity configuration. At the zero angle of attack, no wing-tip vortex was formed for both wing models due to the zero pressure difference between the lower and upper wing surfaces. As the angle of attack increases from 5°-15°, the wing-tip vortex becomes stronger and maturely developed with an inboard circulation over the wing-tip.

Due to the roll-up swirling motion of the wing-tip vortex, the downwash resulted in vortex trapping in the cavity of the wing model. The trapped vortex rotated clockwise before exiting the cavity. The experiment also revealed that vortex trapping occurred more significantly at higher angles of attack for the triple-cavity wing model.

The visualization results also revealed that the core of the wing-tip vortex for the triple-cavity wing model appeared smaller than that of the baseline wing model at angles of attack of 5°, 10° and 15°. This observation suggested that the wing-tip vortex strength is reduced for wing with cavities compared to the non-cavity wing.

Subsequently, it can be deduced that the induced drag for the wing with cavities is smaller than that of the baseline wing, owing to the reduced intensity of the wing-tip vortex for the wing with cavities. Further quantitative study will be required in the future to directly measure the induced drag for this case study.

ACKNOWLEDGEMENTS

The researcher acknowledge financial support from Universiti Sains Malaysia under the Short Term Grant (304.PAERO.60312043) technical supports from Mr. Mohamad Najhan Awang and Mr. Mahmud Isa, wing designs by Ms. Tee Yi Hui and experimental setups by Mr. Anuar M. Nazri from the School of Aerospace Engineering USM.

REFERENCES

- Arndt, R.E.A., V.H. Arakeri and H. Higuchi, 1991. Some observations of tip-vortex cavitation. *J. Fluid Mech.*, 229: 269-289.
- Elsayed, O.A., W. Asrar, A.A. Omar, K. Kwon and H. Jung, 2009. Experimental investigation of wing tip vortex. *Proceedings of the 47th AIAA Conference on Aerospace Sciences Meeting Including the New Horizons Forum and Aerospace Exposition*, January 5-8, 2009, AIAA, Orlando, Florida, pp: 1-8.
- Gerz, T., F. Holzapfel and D. Darracq, 2002. Commercial aircraft wake vortices. *Prog. Aerosp. Sci.*, 38: 181-208.
- Giuni, M. and R.B. Green, 2013. Vortex formation on squared and rounded tip. *Aerosp. Sci. Technol.*, 29: 191-199.
- Liu, Y.C. and F.B. Hsiao, 2012. Aerodynamic investigations of low-aspect-ratio thin plate wings at low Reynolds numbers. *J. Mech.*, 28: 77-89.
- Rossow, V.J., J.N. Sacco, P.A. Askins, L.S. Bisbee and S.M. Smith, 1995. Wind tunnel measurements of hazard posed by lift-generated wakes. *J. Aircr.*, 32: 278-284.
- Sohn, M.H. and J.W. Chang, 2012. Visualization and PIV study of wing-tip vortices for three different tip configurations. *Aerosp. Sci. Technol.*, 16: 40-46.
- Tee, Y.H., 2015. Development of smoke wire system for Vortex trapping application. MA Thesis, Universiti Sains Malaysia, George Town, Malaysia.